The control of pH and ionic strength gradients on the interaction of low-molecular-weight organic acids and siderophores

George H.R. Northover,[1] Yiru Mao,[1] MD Hanif,[1,2] Salvador Blasco,[3] Ramon Vilar,[4] Enrique Garcia-España,[3] and Dominik J. Weiss[1,5]

[1]Department of Earth Science and Engineering, Imperial College London, South Kensington Campus, SW7 2AZ, UK
[2]Soil, Water and Environment Discipline, Khulna University, Khulna 9208, Bangladesh
[3]Instituto de Ciencia Molecular (ICMol), University of Valencia, C/Catedrático José Beltrán Martínez, 2, 46980, Paterna, Valencia, Spain
[4]Department of Chemistry, Imperial College London, White City Campus, W12 0BZ, UK
[5]Department of Civil and Environmental Engineering, Princeton University, New Jersey 08540, USA

Author for correspondence: GN and DW
Telephone number: +44 2075 946383
Email address:
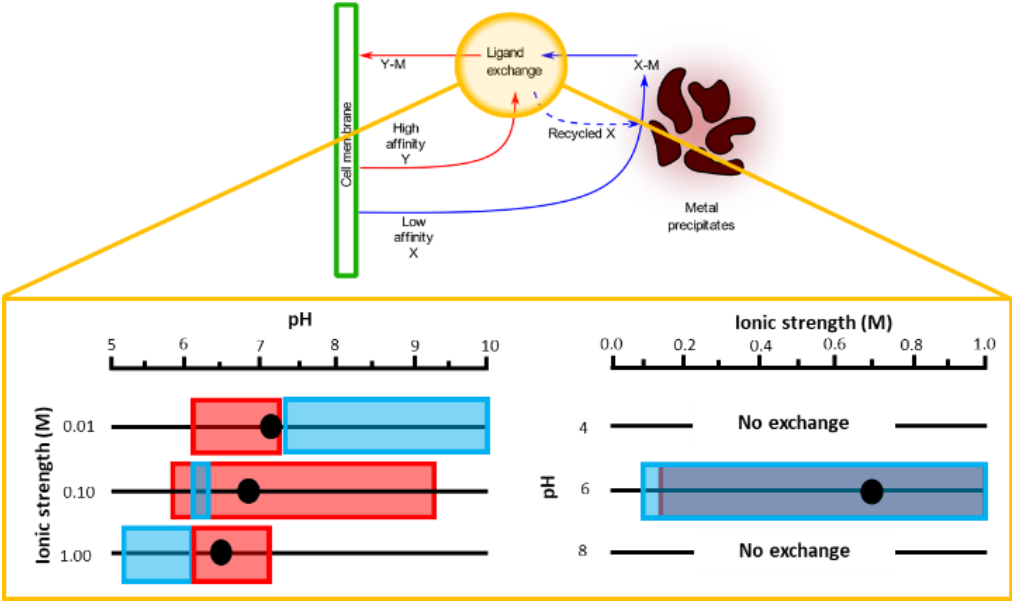george.northover16@imperial.ac.uk;
d.weiss@imperial.ac.uk

Wordcount: 6,125
Figures: 5 figures (Fig. 1, 3, 4, 5 require colour)

39 ## Abstract

40 A wide range of organic ligands are found in the rhizosphere. Two

41 important groups are low-molecular-weight organic acids (LMWOAs)

42 and siderophores. Our understanding of the interaction between co-

43 existing LMWOAs and siderophores during micronutrient cycling in

44 the rhizosphere is limited. Such gaps in our knowledge undermine

45 biofortification efforts. In this study, we test the hypothesis that pH

46 and ionic strength gradients make it possible for LMWOAs and

47 siderophores to function synergistically during micronutrient cycling

48 in the rhizosphere. For this research, we use citrate and

49 desferrioxamine B as our representative LMWOA and siderophore,

50 respectively, and the micronutrient under study is zinc(II). For the first

51 time, we develop an accurate description of the ionic strength

52 dependence of stability constants for a metal/LMWOA and a

53 metal/siderophore system. We then use these ionic strength

54 dependence models to compare the geochemical stability fields of

55 zinc(II)-LMWOA and zinc(II)-siderophore complexes in NaCl. This

56 allows us to predict the ligand interchange points (LIPs) for the

57 exchange of zinc(II) between LMWOAs and siderophores. The

58 predicted LIPs fall within the expected rhizosphere gradients. This

59 supports the idea that pH and ionic strength gradients make it possible

60 for LMWOAs and siderophores to function synergistically during

61 micronutrient cycling in the rhizosphere. Finally, we calculate LIPs for

62 the exchange of zinc(II) between our representative LMWOA and

63 siderophore in model solutions based on the chemistry of rice-growing

64 soils. The LIPs calculated in these model solutions fit with those

65 predicted in NaCl.

66 Graphical abstract

67

68

69 Keywords

70 Low-molecular-weight organic acids (LMWOAs), ionic strength, pH,

71 siderophore, stability constants, zinc(II)

72

73

74

75

76

77

78

79

80

81

82

1. Introduction

There is a diverse range of organic ligands in the rhizosphere (Jones, 1998). Organic ligands found in the rhizosphere can originate from plants, bacteria, or fungi but often function as allelochemicals; a ligand released by one organism may directly or indirectly influence the metal homeostasis of a neighbouring organism, be it of the same species or from a different taxonomic kingdom (Bais et al., 2006; Bertin et al., 2003; Weston et al., 2012). Two important groups of organic ligand that are found in the rhizosphere are low-molecular-weight organic acids (LMWOAs) and siderophores. LMWOAs can be monocarboxylic, dicarboxylic, or tricarboxylic, and generally form weaker complexes with metal ions compared to siderophores. Citrate is a tricarboxylic LMWOA, which is released by many different soil-dwelling organisms. Siderophores are typically hexadentate and bind to a central metal atom with an octahedral coordination (Butler and Theisen, 2010). Increased siderophore secretion is primarily linked to low iron supply (Ahmed and Holmström, 2014). Desferrioxamine B (DFOB) is a hydroxamic siderophore produced by the soil bacterium *Streptomyces pilosus* (Codd et al., 2018). A 3-step model for the complexation of metals by DFOB has previously been proposed, with each of its three hydroxamate groups coordinating to the metal ion in succession as pH increases (Schijf et al., 2015).

Both LMWOAs and siderophores are associated with the cycling of a wide range of biologically important trace metals in the rhizosphere, including zinc (Gries et al., 1998; Marschner, 1988; Rose et al., 2013; Zhang et al., 1991). However, our understanding of the interaction

110   between co-existing LMWOAs (weak) and siderophores (strong)

111   ligands during micronutrient cycling in the rhizosphere is limited; a

112   synergic effect between citrate and DFOB on the dissolution of Mn

113   containing minerals has previously been evidenced in soils (Zhong et

114   al., 2013). Such gaps in our understanding of micronutrient cycling

115   undermine biofortification efforts, which are essential for eradicating

116   hidden hunger and mitigating the potential food security consequences

117   of climate change (Montanarella et al., 2016; Sharma et al., 2017;

118   Wheeler and Braun, 2013). For example, the zinc status of crop plants

119   is a major concern - it is estimated that 1.1 billion people worldwide

120   are at risk of zinc deficiency due to inadequate dietary supplies

121   (Kumssa et al., 2015). Zinc deficiency is particularly prevalent in south

122   Asian populations where rice is a staple food (Akhtar et al., 2013).

123   Both LMWOAs and siderophores have been implicated in zinc

124   acquisition by rice plants (Arnold et al., 2010; Gao et al., 2009;

125   Hoffland et al., 2006; Widodo et al., 2010).

126

127   McRose *et al.* proposed one model for the interaction of weak and

128   strong ligands released by bacteria during iron acquisition in natural

129   solutions (McRose et al., 2018; Figure 1). This model is based upon

130   mineral dissolution mechanism studies in the presence of both types

131   of ligand (Cheah et al., 2003; Reichard et al., 2007). In the McRose *et*

132   *al.* model, the weak ligand (X) adsorbs to the mineral surface and

133   subsequently strips the metal away from the mineral, bringing it into

134   solution. After the formation of a labile MX (where M = metal)

135   complex at the mineral surface, it is proposed that a ligand exchange

136   reaction takes place in which the metal is transferred to the strong

137   ligand (Y) and the weak ligand is free to react with the mineral again.

138 The model is very attractive, however, it leads to the question: what

139 triggers the exchange of the metal ion between X and Y in solution?

140 Physiochemical studies have demonstrated that pH and ionic strength

141 exert a critical influence on metal-ligand interactions in solution (Cao

142 et al., 2004; Cigala et al., 2012; Krężel and Maret, 2016). In previous

143 work, we showed that pH and ionic strength gradients in the root-soil

144 interface zone are a potential controlling factor for the *modus operandi*

145 of organic ligands in the soil environment (Northover et al., 2020).

146 Hence, our theory is that pH and ionic strength gradients make it

147 possible for LMWOAs and siderophores to function synergistically

148 during micronutrient cycling in the rhizosphere.

149

150 The pH of the rhizosphere can vary by more than 2 pH units < 10 mm

151 from the root surface but tends to remain within pH 5.5 – 8.5 regardless

152 of the mineralogical composition of the parent material (Bravin et al.,

153 2009; Gollany and Schumacher, 1993; Kirk, 1993). The ionic strength

154 of soil solutions which are unaffected by salinity contamination is

155 ~0.005 M (Black and Campbell, 1982; Dolling and Ritchie, 1985;

156 Edmeades et al., 1985). Due to sampling difficulties, it has not yet been

157 possible to measure ionic strength gradients in the rhizosphere.

158 Simulated rhizosphere solute concentration profiles, for soils with a

159 variety of different properties, suggest that the concentration of root

160 exudates increases between five- to 10-times < 2.5 mm from the root

161 surface (Raynaud, 2010). Assuming that the ionic strength gradient

162 parallels the solute concentration gradient (which holds if anion/cation

163 pairs are predominantly singularly charged), rhizosphere ionic

164 strength is expected to range between 0.005 – 0.05 M. The first step

165 towards testing the hypothesis that pH and ionic strength gradients in

166   the rhizosphere make it possible for LMWOAs and siderophores to

167   function synergistically during micronutrient cycling in the

168   rhizosphere involves using equilibrium (geochemical) speciation

169   modelling tools to compare the pH and ionic strength stability fields

170   for metal-LMWOA and metal-siderophore complexes in a simple

171   aqueous solution. Metal complexation to inorganic and organic ligands

172   in solution is relatively fast, therefore, kinetics are not relevant (Di

173   Bonito et al., 2018). If the pH and/or ionic strength at which metal-

174   siderophore complexes become more stable than metal-LMWOA

175   complexes (or *vice versa)* falls within the boundaries of the respective

176   gradients expected in the rhizosphere, this would provide an initial

177   piece of supporting evidence for the hypothesis as it would imply that

178   the two types of metal-ligand complex dominate in different parts of

179   the rhizosphere.

180

181   Geochemical speciation modelling relies only on knowing the

182   concentrations of elements in the study, the species that could form

183   (the equilibrium model), and the stability constants for the associated

184   complexation reactions. Stability constants calculated at standard state

185   (*i.e.*, 298.15 K, 1 atm, infinite dilution), where concentrations are equal

186   to activities, are known as intrinsic stability constants ($\log \beta^0$).

187   Stability constants measured at any other conditions are conditional

188   ($\log \beta$), their value depends on the chemical and physical conditions

189   (ionic strength, temperature, and pressure) under which they were

190   measured (Cigala et al., 2015a, 2013). To delineate the ionic strength

191   stability field for metal-LMWOA and metal-siderophore complexes,

192   we need to know stability constants at many different ionic strengths

193   within an environmentally relevant sampling range (*i.e.,* 0 – 1 M) in

194 the same electrolyte. However, to our knowledge, no study reports

195 either metal-LMWOA or metal-siderophore stability constants at more

196 than two ionic strengths in the same electrolyte. Although it would be

197 possible to create a dataset by bringing together stability constants

198 measured in different studies, ionic strength-driven changes in log β

199 can be small compared to laboratory error and so it is not advisable to

200 combine data from independent studies. Filling in missing data points

201 by adjusting experimental stability constants using calculated activity

202 coefficients (indirect method) also has several limitations (Northover

203 et al., 2020). The gold standard for studying the ionic strength

204 dependence of stability constants is to use a direct method *i.e.,* without

205 calculating activity coefficients. Direct methods are highly accurate

206 and easy to apply. They involve measuring stability constants at a

207 limited number of points within the ionic strength range of interest and

208 then fitting a modified version of the Extended Debye-Hückel

209 equation (Equation 1) or specific ion interaction theory to the

210 experimental data series (Bretti et al., 2006, 2004; Cigala et al., 2012).

211 $$\log \beta^0 = \log \beta - 0.51 z^* \frac{\sqrt{I}}{1 + 1.5\sqrt{I}} + f(I)$$

212 (1)

213 where z is the charge of the ion, $z^* = \Sigma(z^2_{react}) - \Sigma(z^2_{prod})$, I is ionic

214 strength (M), and $f(I)$ is a linear function of ionic strength that can be

215 formulated in different ways. The simplest expression for this term is

216 $f(I) = CI$, where C is the only adjustable parameter. Usually, this

217 simple choice is sufficient to explain the experimental data trend in a

218 wide ionic strength range, generally < 1.0 M.

219

220   The aim of this study is to test the hypothesis that pH and ionic strength

221   gradients make it possible for LMWOAs and siderophores to function

222   synergistically during micronutrient cycling in the rhizosphere. For

223   this research, we use citrate and DFOB as our representative LMWOA

224   and siderophore, respectively, and the micronutrient under study is

225   zinc(II).

226   (i)   To begin, we study the ionic strength dependence of

227   zinc(II)-citrate and zinc(II)-DFOB stability constants

228   using a direct approach. We measure $\log \beta$ values at

229   multiple ionic strengths in NaCl and then fit a

230   modified version of the Extended Debye-Hückel

231   equation to the data. This is the first time an accurate

232   description of the ionic strength dependence of

233   stability constants has been developed for either a

234   metal/LMWOA or a metal/siderophore system and is

235   a pre-requisite for the subsequent stages of the

236   investigation.

237   (ii)   We then model the speciation of our representative

238   zinc(II)/LMWOA and zinc(II)/siderophore systems at

239   standard [Zn] and [L] (where L = ligand) conditions

240   as a function of pH and ionic strength in NaCl. This

241   allows us to predict the pH and ionic strength ligand

242   interchange points (LIPs) for the exchange of zinc(II)

243   between LMWOAs and siderophores. Comparing the

244   predicted LIPs to the geochemical gradients expected

245   in the rhizosphere enables a preliminary test of our

246   hypothesis. We draw comparisons between the pH

247   complexation curves for the zinc(II)/citrate and

248		zinc(II)/DFOB systems with other zinc(II)/LMWOA
249		and zinc(II)/siderophore systems reported in the
250		literature to justify the use of these two ligands as
251		representatives for their respective groups.
252	(iii)	Finally, we calculate the LIPs for the exchange of
253		zinc(II) between our representative LMWOA and
254		siderophore in model solutions based on the chemistry
255		of rice-growing soils. The question we want to answer
256		is: does the position of the LIPs change in real soil
257		solutions? If so, what controls this?
258		
259		
260		
261		
262		
263		
264		
265		
266		
267		
268		
269		
270		
271		
272		
273		
274		
275		

2. Materials and methods

2.1. Chemicals

Zinc(II) solutions were prepared by dissolving the corresponding mass of $ZnCl_2$ (99%, anhydrous, VWR) in water; the concentration was determined by complexometric titration against ethylenediaminetetraacetic acid (EDTA) standard solutions (Fisher Scientific). Standard hydrochloric acid (HCl) solutions were prepared from concentrated HCl (Sigma-Aldrich-Honeywell) and standardized with tris(hydroxymethyl)aminomethane (THAM) (Roche Diagnostics). CO_2-free sodium hydroxide (NaOH) standard solutions were supplied by Fisher Scientific and were preserved from atmospheric CO_2 by means of soda lime traps. Electrolyte solutions of sodium chloride (NaCl) were prepared from the pure salt (VWR). Citric acid monohydrate (VWR) and desferrioxamine mesylate salt (Sigma-Aldrich) powders were used to prepare ligand solutions. Ultrapure water (R = 18 $M\Omega$ cm^{-1}), grade A glassware, and analytical grade reagents were used throughout.

2.2. Determination of stability constants

2.2.1 Potentiometric titrations

Potentiometric measurements were carried out at $T = 298.1 \pm 0.1$ K in thermostated cells. The setup consisted of a Metrohm model 888 Titrando apparatus controlled by Metrohm TiAMO 1.2 software equipped with a combined gel electrode (VWR model 662 1759). Estimated precision was 0.2 mV and 0.003 mL for the electromotive force and titrant volume readings, respectively. All the potentiometric

303   titrations were carried out under magnetic stirring and bubbling

304   purified presaturated N_2 through the solution to exclude O_2 and CO_2.

305

306   Before studying the zinc(II)/ligand systems, the acidity constants of

307   the ligand (pK_a) were determined at different ionic strengths ($0.05 \leq$

308    $M \leq 1.00$) in NaCl solutions. A 30 mL solution containing each ligand

309   ([L] = 5 mM), NaCl and HCl was titrated with standard NaOH

310   solutions. For the zinc(II)/ligand systems, the titrant solutions

311   consisted of different concentrations of ligand ([L] = 1 to 5 mM),

312   zinc(II) ([Zn] = 0.5 to 1.5 mM), a suitable amount of HCl and NaCl.

313   All the measurements were carried out with an excess of the ligand,

314   with respect to the concentration of the zinc(II) and in different zinc:

315   ligand molar ratios (0.9:1 and 1:2). Zinc(II) and ligand concentrations

316   were negligible compared to the background electrolyte. Calculations

317   showed that ionic strength remained within 10% (v/v) of the targeted

318   value throughout all titrations.

319

320   For each experiment, independent titrations of strong acid solutions

321   with standard base were carried out under the same medium and ionic

322   strength as the systems to be investigated, with the aim of determining

323   the electrode potential (E^0) using GLEE software (Gans and

324   O'Sullivan, 2000). In this way, the pH scale used was the total scale,

325   pH = -log [H^+], where [H^+] is the free proton concentration. For each

326   titration, approximately 80 to 100 data points were collected, and the

327   equilibrium state during titrations was checked by confirming the time

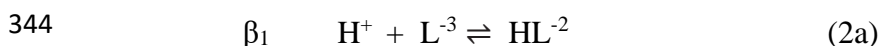328   required to reach equilibrium.

329

330   2.2.2 Calculating stability constants from titration data

331   Hyperquad was used to determine the equilibrium model and to

332   calculate acidity and stability constants from the potentiometric data

333   set (Gans et al., 1996). For each set of ligand acidity constants or

334   zinc(II): ligand ratio, at least two different titrations were performed.

335   The titration curves for each system were treated as a single set when

336   refining stability constants. This meant that the refinement procedure

337   was run on both curves at the same time to derive a single set of

338   constants. The error reported on the stability constants is the standard

339   deviation given in the Hyperquad output file.

340

341   In Hyperquad, stability constants are defined as overall association

342   constants (β). For a polyprotic acid (H_3L) with three acidic sites, the β

343   constants are defined as:

344
$$\beta_1 \qquad H^+ + L^{-3} \rightleftharpoons HL^{-2} \qquad\qquad (2a)$$

$$\beta_2 \qquad 2H^+ + L^{-3} \rightleftharpoons H_2L^{-1} \qquad\qquad (2b)$$

$$\beta_3 \qquad 3H^+ + L^{-3} \rightleftharpoons H_3L \qquad\qquad (2c)$$

345   Stepwise stability constants (K) are obtained from overall constants

346   using the rule:

347
$$\beta_2 = K_1 K_2 \qquad\qquad (3)$$

348

349   In this study, the ionic strength dependence of the formation constants

350   was studied with the extended Debye–Hückel type model (Bretti et al.,

351   2006). The Monte Carlo method, as described by Hu *et al.*, was used

352   to estimate 95% confidence intervals on the parameters of ionic

353   strength dependence; for each species, predicted stability constants

354   were resampled using an inverse of the cumulative normal distribution

355   function to give sets of simulated data from which the unknown

356   parameters were optimized (W. Hu et al., 2015). Examples of manual

357   fitting plots from Hyperquad are included in the supporting

358   information (Figure S1 and S2). In addition to the supporting

359   information provided in this publication, example hyperquad files (for

360   both the zinc(II)/citrate and zinc(II)/DFOB systems) and example

361   Excel calculation files for the application of the Modified Debye-

362   Huckel equation to the zinc(II)/DFOB system (including the

363   calculation of error on parameters of ionic strength dependence) have

364   been   uploaded   to   the   Zenodo   repository   (DOI:

365   10.5281/zenodo.4548162). In **3.1.**, the Davies equation (Equation 4) is

366   applied to the zinc(II)/citrate data to facilitate a comparison between

367   direct and indirect methods of studying ionic strength dependence. The

368   Excel calculation file associated with this task is also available on the

369   Zenodo repository (DOI: 10.5281/zenodo.4548162).

370    $$-\log \gamma_i = -Az_i^2 \left\{ \frac{\sqrt{I}}{1 + \sqrt{I}} - 0.3I \right\} \qquad (4)$$

371   where A is a dielectric constant of the solvent, z is the charge of the

372   ion, and I is ionic strength (M).

373

374   **2.3. Speciation modelling**

375   Speciation calculations in **3.1.** and **3.2.** were conducted with the aid of the

376   Hyperquad Simulation and Speciation computer software (HySS) utilizing

377   stability constants and the ionic strength dependence relationships

378   determined in the preceding phase of the study (Alderighi et al., 1999). For

379 all speciation calculations, $[Zn] = 10^{-6}$ M and $[L] = 10^{-5}$ M. These $[Zn]$

380 and $[L]$ conditions are the standard concentrations adopted by

381 bioinorganic chemists studying the effectiveness of ligands (Harris et

382 al., 1981). The error on speciation plots in **3.1.** was determined by re-

383 running the analysis, starting with the high/low estimates for the

384 experimental stability constants. The error on speciation calculations

385 in **3.2.** was investigated by re-running the analysis using the high/low

386 estimates for the parameters of ionic strength dependence. The error

387 on the speciation calculations in **3.2.** is not reported in the associated

388 tables and figures as it was extremely small and had no significance

389 for the interpretations of the results; pH and ionic strength LIPs shifted

390 by < 0.01 pH units and < 0.001 M, respectively.

391

392 Speciation calculations in **3.3.** were produced with the aid of Visual

393 MINTEQ and the NICA-Donnan model (Gustafsson, 2013; Milne et

394 al., 2003). The NICA-Donnan model is a combination of the non-ideal

395 competitive adsorption isotherm (NICA), which describes the binding

396 of heterogeneous material, and a Donnan electrostatic sub-model,

397 which describe the electrostatic interactions between ions and humic

398 material (Milne et al., 2003). Two model solutions, Solution A and

399 Solution B, were created based on the chemistry of rice-growing soils

400 in south-western Bangladesh; since rice is cultivated in flooded soils

401 and groundwater is used for irrigation, the composition of soil

402 solutions was assumed to be closely related to that of the groundwater

403 (Ahmed et al., 2020; Ayers et al., 2016; Bahar and Reza, 2010; Hug et

404 al., 2008). Rice-growing soils were selected for study because of the

405 importance of zinc biofortication of rice (high prevalence of zinc

406 deficiency of South Asian populations for whom rice is a staple food)

407	and the proposed role for both LMWOAs and siderophores during zinc
408	cycling in the rhizosphere of rice plants. The concentration of
409	dissolved organic matter used in the solutions was 3.3 mM. The
410	concentration of fulvic acids containing carboxylic and phenolic
411	groups were 0.38 and 0.12 mM, respectively. The concentration of
412	zinc(II) was set at 0.08 mM , this is a high estimate for zinc(II)
413	concentration and reflects the widespread use of fertilizers in crop
414	production in Bangladesh (Bhowmick et al., 2014; Siddique and
415	Abdullah, 2015). The two solutions were differentiated by the
416	concentration of bicarbonate ions; Solution A = 2 mM and Solution B
417	= 8 mM. Different sets of LMWOA (citrate) and siderophore (DFOB)
418	concentrations were analysed in each of the solutions. The LMWOA
419	and siderophore concentrations tested ranged between 1 – 50 µM and
420	0.1 – 1 µM, respectively (Jones et al., 2003; Powell et al., 1980;
421	Ptashnyk et al., 2011). Stability constants for aqueous inorganic
422	species (zinc-chloride, zinc-carbonate, zinc-hydroxide, *etc*.) were
423	taken from the default database in Visual MINTEQ, this database is
424	primarily based on the National Institute of Standards and Technology
425	(NIST) compilation (Smith et al., 2004). The stability constants
426	determined in this study for citrate and DFOB species were added to/or
427	amended in the database. The stability constants stored in the database
428	for citrate and DFOB species were adjusted when running the model
429	at each new ionic strength so that the inbuilt Davies function used in
430	Visual MINTEQ would set log β at the desired value (*i.e.*, the
431	conditional value predicted by the appropriate modified Debye-Huckel
432	model from this study). pH and ionic strength were both fixed in
433	Visual MINTEQ, rather than calculated. LIPs were calculated by
434	determining the pH or ionic strength condition at which the

435   concentration of zinc(II)-siderophore and zinc(II)-citrate complexes

436   were equal. Visual MINTEQ template files for the solutions – not

437   including the LMWOA and siderophore components - are available on

438   the Zenodo repository (DOI: 10.5281/zenodo.4548162).

439

440

441

442

443

444

445

446

447

448

449

450

451

452

453

454

455

456

457

458

459

460

461

462

3. Results and discussion

3.1. Determination of equilibrium models, stability constants, and parameters ($\log \beta^0, C$) of ionic strength dependence

Values of acidity constants for citrate and DFOB at different ionic strength in NaCl and $T = 298.1$ K are reported in Table 1 with the parameters of ionic strength dependence. Experimental and modelled zinc(II)-ligand stability constants are presented in Figure 2 with literature data. Comprehensive results for the zinc(II)/ligand systems, including stability constants for hydrolysed zinc(II)-ligand species are reported in Table S1.

The errors reported on the measured acidity/stability constants and log β^0 are too small to have a measurable effect on subsequent speciation calculations. The error reported on C is larger than in similar studies (Cigala et al., 2012). A sensitivity analysis on the three zinc(II)-ligand species with the largest relative error on C, finds that where log β^0 is recalculated for the maximum/minimum possible C values, log β^0 remains within its error range. Hence, the error on C does not affect the accuracy of log β^0.

The stability constants reported in the literature for the zinc(II)/citrate system are inconsistent (Capone et al., 1986; Cigala et al., 2015b; Daniele et al., 1988; Field et al., 1975; Li et al., 1959; Matsushima, 1963). For example, the stability constant reported for [ZnCit]$^-$ in 0.1 M KNO$_3$ varies by 1.36 log units (Capone et al., 1986; Field et al.,

490 1975). The stability constant we report for [ZnCit]⁻ in 0.15 M NaCl

491 shows good agreement with that reported by Cigala *et al.* in 0.15 M

492 NaCl; 4.66 vs. 4.71 (Cigala et al., 2015a). The equilibrium model that

493 gave the best statistical fit and chemically sensible values included one

494 zinc(II)-citrate species which has not previously been identified,

495 namely; $[Zn(OH)_3Cit]^{4-}$, which exists only above pH 9. However, it

496 did not include $[ZnCit_2]^{4-}$, a species that has been identified in previous

497 studies (Cigala et al., 2015b). We could detect the formation of

498 $[ZnCit_2]^{4-}$ but could not refine the stepwise stability constant (K) for

499 the complex to within +/- 0.09 log units. Indicating that it is an unstable

500 species that forms at negligible concentrations under the conditions

501 examined. The stability constants for citrate complexation with

502 zinc(II) decrease with increasing ionic strength. The most significant

503 change is seen between 0.05 – 0.15 M NaCl, where there is

504 approximately a 0.5 – 1.5 log unit change in the stability constants. In

505 dilute solutions stability constants are sensitive to small increases in

506 ionic strength because changes in the effective concentration (activity)

507 of ions are large.

508

509 For the zinc(II)/DFOB system, the stability constants measured in this

510 study are in good agreement with those reported in the literature

511 (Farkas et al., 1997; Hernlem et al., 1996; Schijf et al., 2015). For

512 example, the stability constant we report for [ZnHDFOB] at 0.5 M

513 NaCl is 19.34. This is within ~0.5 log units of the stability constant

514 reported by Schijf *et al.* 0.7 M in NaClO₄ (Schijf et al., 2015). The

515 speciation scheme we report differs slightly from that predicted based

516 on the three-step model. Our equilibrium model does not include the

517 bidentate species $([ZnH_3DFOB]^{2+})$, the weakest and least stable

518 zinc(II)-DFOB species we might expect to find. Instead in Table S1

519 we report stability constants for two hexadentate species ([ZnDFOB]$^-$

520 and [ZnHDFOB]) and one tetradentate species ([Zn H$_2$DFOB]$^+$). We

521 observe that as the denticity of the complex increases, so does the

522 strength of the stability constant. The stepwise stability constant (K)

523 differs by approximately 2 log units between the bidentate and

524 hexadentate species. Two hexadentate species exist because at low pH

525 the terminal amine group which does not participate in the binding is

526 protonated. DFOB complexation of zinc(II) shows the same pattern of

527 ionic strength dependence as citrate, with the greatest decrease in the

528 constants occurring between 0.05 – 0.15 M NaCl. The absolute

529 decrease in [ZnL] and [ZnHL] stability constants between 0.05 - 0.15

530 M is approximately equal for citrate and DFOB species (average 1.58

531 vs. 1.73). This makes sense given that the effect of ionic strength

532 primarily depends on the charge of the ions involved and free citrate

533 and DFOB have the same electrostatic charge (-3). The ionic strength

534 dependence parameter C shows no systematic change for either citrate

535 or DFOB species.

536

537 In Figure 3a intrinsic stability constants for the formation of [ZnCit]$^-$

538 and [ZnHCit] species determined at different ionic strengths using the

539 Davies equation are compared to the intrinsic stability constants for

540 the same two species determined by fitting the modified version of the

541 Extended Debye-Hückel equation to the full ionic strength dataset.

542 Intrinsic stability constants for the full zinc(II)/citrate system

543 calculated using the Davies equation are reported in Table S2. Figure

544 3b shows the fraction of complexed zinc(II) in a zinc(II)/citrate system

545   modelled at infinite dilution using intrinsic stability constants

546   determined (i) directly, by fitting the modified version of the Extended

547   Debye-Hückel equation to the full citrate (pK_a and zinc(II)-citrate)

548   stability constant dataset (ii-vi) indirectly, using the Davies equation

549   to calculate activity coefficients and adjust the citrate (pK_a and

550   zinc(II)-citrate) stability constants separately at 0.05, 0.15, 0.30, 0.50,

551   and 1.00 M. At pH 5.5, the 0.05 M Davies-based intrinsic speciation

552   model overpredicts the fraction of complexed zinc(II) by

553   approximately 20% compared to the Extended Debye-Hückel-based

554   intrinsic speciation model. At the same pH value, the 0.15, 0.3, 0.5,

555   and 1 M Davies-based intrinsic speciation models underpredict the

556   fraction of complexed zinc(II) by 18, 21, 20, and 38%, respectively,

557   compared to the Extended Debye-Hückel-based intrinsic speciation

558   model. Firstly, this exercise clearly demonstrates the inconsistencies

559   in speciation calculations that can arise when the same geochemical

560   model is run using different sets of stability constants derived by

561   applying the same indirect method (Davies equation) to different sets

562   of ionic strength data; even when the different sets of ionic strength

563   data are within the activity model's supposed ionic strength range of

564   applicability (for Davies equation < 0.5 M *i.e.*, 0.05, 0.15, and 0.3 M)

565   and from the same study. Secondly, this exercise quantifies the

566   improvement in the accuracy of geochemical speciation calculations

567   that can be achieved by adopting a direct method for studying the ionic

568   strength dependence of stability constants, rather than using an indirect

569   method, as is the common practise.

570

571   In this section, for the first time, we have developed an accurate

572   description of the ionic strength dependence of stability constants for

573   a metal/LMWOA and a metal/siderophore system. We have

574   quantified the benefits of the direct approach for studying the ionic

575   strength dependence of stability constants; when the zinc(II)/citrate

576   system is modelled at infinite dilution using high precision intrinsic

577   stability constants determined using a direct approach, the accuracy

578   of geochemical speciation calculations improves by at least 18% at

579   pH 5.5 compared to when the Davies equation is used instead to

580   calculate intrinsic stability constants..

581

582   **3.2. Identification of LIPs for the exchange of zinc(II)**

583   **between LMWOAs and siderophores in NaCl solutions**

584   The ionic strength dependence models described above were

585   subsequently applied to investigate the geochemical stability field of

586   the metal/ligand systems of interest. Figure 4 shows the fraction of

587   complexed zinc(II) in our representative zinc(II)/LMWOA (citrate)

588   and zinc(II)/siderophore (DFOB) systems as a function of **(a)** pH and

589   **(b)** ionic strength in NaCl solutions. The raw data for these plots are

590   supplied in the supporting information (Table S3-S4).

591

592   3.2.1. pH stability field of zinc(II)-LMWOA and zinc(II)-siderophore
593   complexes
594   For both the zinc(II)/LMWOA and zinc(II)/siderophore systems, the

595   fraction of complexed zinc(II) increases with pH. For all ionic

596   strengths examined, zinc(II)-LMWOA complexes begin forming at

597   approximately pH 3. Once the LMWOA begins binding to zinc(II), it

598   takes between 6 - 7 pH units to reach total zinc(II) complexation in the

599   zinc(II)/LMWOA system. The fraction of zinc(II) complexed by the

600   LMWOA increases fastest with pH in the lowest ionic strength

601   solution. At pH 6 in the 0.01 M solution, the fraction of zinc(II)

602   complexed by the LMWOA is 0.81. This is compared to just 0.07 at

603   the same pH in the 1 M solution. The formation of zinc(II)-LMWOA

604   complexes does not increase continuously with pH, there is a 2 – 3 pH

605   unit plateau in the pH complexation curves for the zinc(II)/LMWOA

606   system. Speciation diagrams for zinc(II)/malate and zinc(II)/tartrate

607   systems available in the literature show a similar trend to the

608   zinc(II)/LMWOA pH complexation curves in this study; significant

609   formation of zinc(II)-malate/tartrate complexes (> 10% fraction of

610   total zinc) occurs at around pH 2 - 3 and there is then a plateau/only a

611   small increase in the formation of zinc(II)-malate/tartrate complexes

612   between pH 5 – 7 (Cigala et al., 2015a). The similarities in the pH

613   complexation curves for the different LMWOAs endorses the use of

614   citrate as a general LMWOA representative in this study. In the

615   zinc(II)/siderophore system, ionic strength has a negligible effect on

616   the pH complexation curves. In all solutions, complexation of zinc(II)

617   begins at pH 5.5 and total zinc(II) complexation is reached within 3

618   pH units; no free zinc(II) remains in the zinc(II)/siderophore systems

619   above pH 8. The pH complexation curves for the zinc(II)/siderophore

620   system are sigmoidal and do not contain a plateau. Speciation

621   diagrams for the zinc(II)/deoxymugineic acid (DMA) system show a

622   similar pattern to the zinc(II)/siderophore pH complexation curves in

623   this study; DMA is a plant-produced siderophore (Weiss *et al.*, 2021).

624   Significant concentrations of zinc-DMA complexes begin forming at

625   around pH 5 and total complexation of zinc(II) is completed within 1.5

626   pH units. The similarities in the pH complexation curves between the

627   two zinc(II)/siderophore systems endorses the use of DFOB as a

628   general siderophore representative in this study.

629

630   The pH at which zinc(II)-siderophore complexes become more stable

631   than zinc(II)-LMWOA complexes (*i.e.,* the fraction of complexed

632   zinc(II) in the zinc(II)/siderophore system becomes greater than the

633   fraction of complexed zinc(II) in the zinc(II)/LMWOA system),

634   depends on ionic strength. As ionic strength increases the pH LIP

635   becomes more acidic. In the 0.01, 0.1, and 1 M solutions, the pH LIP

636   is at pH 7.5, 7.1, and 6.5, respectively. This suggests that the

637   thermodynamic favourability of the reaction for the exchange of

638   zinc(II) between LMWOAs and siderophores increases with ionic

639   strength. Assuming there are two solutions buffered at the same pH,

640   which contain identical concentrations of zinc(II) and LMWOA, if an

641   equal amount of siderophore was added to each solution and they are

642   allowed to reach equilibrium, based on our modelling analysis we

643   would predict that the solution which has the higher ionic strength

644   would contain greater concentrations of zinc(II)-siderophore

645   complexes. The thermodynamic effect of ionic strength on ligand

646   exchange between LMWOAs and siderophores we infer conflicts with

647   the kinetic effect of ionic strength on the ligand exchange rate between

648   citrate and DFOB previously observed. There is evidence that the

649   ligand exchange rate between citrate and DFOB increases at lower

650   ionic strengths (Ito et al., 2015).

651

652 For all ionic strengths tested, the predicted pH LIPs (pH 6.5 - 7.5) fall

653 within the pH gradients expected in a typical rhizosphere (2 pH units

654 between pH 5.5 – 8.5). This supports the idea that pH gradients make

655 it possible for zinc(II)-LMWOA and zinc(II)-siderophore complexes

656 to dominate in different parts of the rhizosphere and, therefore, for the

657 ligands to function synergistically.

658

659 3.2.2. Ionic strength stability field for zinc(II)-LMWOA and zinc(II)-
660 siderophore complexes

661 As ionic strength increases, the stability of zinc(II)-LMWOA

662 complexes decreases. Between 0 - 1 M, the fraction of zinc(II)

663 complexed by LMWOA decreases by 0.05, 0.84, and 0.89 at pH 4, 6,

664 and 8, respectively; in all instances this represents a relative reduction

665 in ligand binding efficiency of approximately 92%. The zinc(II)-

666 LMWOA ionic strength complexation curves initially descend

667 sharply, two-thirds of the reduction in binding efficiency occurs before

668 0.2 M. For zinc(II)-siderophore complexes, ionic strength only has an

669 effect on stability at pH 6. At pH 4, no zinc(II)-siderophore complexes

670 are stable and at pH 8 zinc(II) is fully complexed by the siderophore

671 at all ionic strengths. At pH 6, between 0 - 1 M, the decrease in fraction

672 of complexed zinc(II) is 0.09 in the zinc(II)/siderophore system. This

673 represents a relative reduction in ligand binding efficiency of 45%.

674 Hence, the effect of ionic strength is more important for the stability

675 of zinc(II)-LMWOA complexes than the stability of zinc(II)-

676 siderophore complexes; it is larger (relative reduction in ligand

677 binding efficiency 92% vs. 45%) and it is relevant over a wider pH

678 range.

679

680   The ionic strength LIP at pH 6 is approximately 0.7 M. At pH 4, the

681   LMWOA remains dominant over the siderophore up to 1 M and at pH

682   8, the siderophore is already dominant over the LMWOA at 0 M. This

683   suggests that the ionic strength LIP occurs at a lower ionic strength as

684   pH increases and consequently that the thermodynamic favourability

685   of the reaction for the exchange of zinc(II) between LMWOAs and

686   siderophores increases with pH. Assuming there are two solutions at

687   the same ionic strength, which contain identical concentrations of

688   zinc(II) and LMWOA, if an equal amount of siderophore was added

689   to each solution and they are allowed to reach equilibrium, based on

690   our modelling analysis we would predict that the solution which has

691   the higher pH would contain greater concentrations of zinc(II)-

692   siderophore complexes. The thermodynamic effect of pH on ligand

693   exchange between LMWOAs and siderophores we infer conflicts with

694   the kinetic effect of pH on the ligand exchange rate between two

695   siderophores previously observed. There is evidence that the ligand

696   exchange rate between siderophores can be increased by acidification

697   of the medium (Tufano and Raymond, 1981).

698

699   Between pH 6 – 8, the predicted ionic strength LIP is < 0.7 M.

700   Additional calculations reveal that between pH 7 - 7.5, the predicted

701   ionic strength LIP ranges from 0.01 – 0.1 M, this overlaps with the

702   estimated ionic strength gradient for a typical rhizosphere (0.005 –

703   0.05 M). Hence, our calculations suggest that when the pH of the

704   rhizosphere is circumneutral, ionic strength gradients make it possible

705   for zinc(II)-LMWOA and zinc(II)-siderophore complexes to dominate

706   in different parts of the rhizosphere and, therefore, for the ligands to

707   function synergistically.

708

709   In summary, this preliminary test of our hypothesis – comparing pH

710   and ionic strength stability fields for zinc(II)-LMWOA and zinc(II)-

711   siderophore complexes in a simple aqueous solution using standard

712   concentrations for [Zn] and [L] – supports the idea that pH and ionic

713   strength gradients make it possible for LMWOAs and siderophores to

714   function synergistically during micronutrient cycling in the

715   rhizosphere. In the next section, we calculate the LIPs for the exchange

716   of zinc(II) between our representative LMWOA and siderophore in

717   model solutions based on the chemistry of rice-growing soils.

718

719   **3.3. The effect of real soil solutions on the position of LIPs**

720   In Figure 5, calculated LIPs are reported for the exchange of zinc(II)

721   between our representative LMWOA and siderophore in two model

722   solutions based on the chemistry of rice-growing soils. The predicted

723   LIPs from the analysis in NaCl using standard [Zn] and [L] are

724   included in the figure for the purpose of comparison. The LIPs

725   calculated for solution A and B are reported as ranges because

726   different sets of LMWOA (1 – 50 µM) and siderophore (0.1 – 1 µM)

727   concentrations were analysed in each of the solutions.

728

729   At all ionic strengths tested, the pH LIPs predicted in NaCl fall outside

730   the range calculated for pH LIPs in solution A. However, the

731   magnitude of this offset is small; 0.2, 0.5, and 0.3 pH units at 0.001,

732   0.1, and 1 M, respectively. At all ionic strengths tested, the pH LIPs

733   predicted in NaCl fall within the range calculated for the pH LIPs in

734   solution B. In accordance with the analysis in **3.2.2.**, it was not possible

735   to calculate ionic strength LIPs in either solution A or B at pH 4 or 8.

736   This is because for all LMWOA and siderophore concentrations tested,

737   at pH 4 LMWOA remained dominant between 0 – 1 M and at pH 8 the

738   siderophore remained dominant between 0 – 1 M. The ionic strength

739   LIP predicted in NaCl at pH 6 falls within the range calculated for the

740   ionic strength LIPs in solution A and B.

741

742   The pH LIPs calculated in solution A and B at individual ionic

743   strengths vary by between 0.2 – 3.4 pH units depending on the

744   concentrations of LMWOAs and siderophores used in the speciation

745   calculations. The ionic strength LIPs vary by between 0.8 – 0.85 M,

746   depending on the concentrations of LMWOAs and siderophores used

747   in the speciation calculations. This evidence suggests that the LIPs in

748   real soil solutions are sensitive to the ligand concentration ratio.

749   Previous investigations have highlighted the ligand concentration ratio

750   as an important factor controlling the ligand-exchange process (Z. Hu

751   et al., 2015). The pH LIPS for solution A and B are not consistent. For

752   example, at 1.00 M, the pH LIP in solution A and solution B are 5.2 -

753   6.1 and 6.1 – 9.1, respectively. There does not appear to be any

754   systematic trend in the discrepancies between the pH LIPs in solution

755   A and B (the pH LIP for solution A is not always lower than the pH

756   LIP for solution B or *vice versa*). The two model solutions are

757   differentiated by the concentration of bicarbonate ions; solution A = 2

758   mM and solution B = 8 mM. Hence, the discrepancies between pH

759   LIPs in solution A and B would imply that the pH LIPs are sensitive

760   to bicarbonate concentration. Bicarbonate ions form complexes with

761   zinc(II) that are stable at high pH (Powell et al., 2005). Competition

762   between the bicarbonate ions and ligands for zinc(II) shifts the position

763 of the LIP. The effect of bicarbonate ion concentration on the ionic

764 strength LIPs at pH 6 appears to be minimal. This is because at pH 6,

765 the ionic strength LIPs are so highly sensitive to ligand concentration

766 ratio that the concentration of bicarbonate ions is made almost

767 irrelevant.

768

769 In summary, the LIPs calculated in the model solutions fit with those

770 predicted in NaCl and largely fall within the range of the expected

771 rhizosphere gradients. As such, our evidence suggests that pH and

772 ionic strength gradients make it possible for LMWOAs and

773 siderophores to function synergistically during zinc cycling in the

774 rhizosphere of rice plants. We also find evidence that in real soil

775 solutions, LIPs are sensitive to both ligand concentration ratios and

776 bicarbonate ion concentration.

777

784

6. Author contribution

786 The experimental data was collected and analysed by GHRN, AM,

787 SB, and EGE. Modelling was conducted by GHRN and MH. The

788 manuscript was written by GHRN after discussions with all authors.

8. References

789 Ahmed, A., Ghosh, P.K., Hasan, M., Rahman, A., 2020. Surface and
790   groundwater quality assessment and identification of hydrochemical
791   characteristics of a south-western coastal area of Bangladesh.
792   Environmental Monitoring and Assessment 192, 1–15.
793   doi:10.1007/s10661-020-8227-0
794 Ahmed, E., Holmström, S.J.M., 2014. Siderophores in environmental
795   research: Roles and applications. Microbial Biotechnology 7, 196–
796   208. doi:10.1111/1751-7915.12117
797 Akhtar, S., Ismail, T., Atukorala, S., Arlappa, N., 2013. Micronutrient
798   deficiencies in South Asia - Current status and strategies. Trends in
799   Food Science and Technology. doi:10.1016/j.tifs.2013.02.005
800 Alderighi, L., Gans, P., Ienco, A., Peters, D., Sabatini, A., Vacca, A., 1999.
801   Hyperquad simulation and speciation (HySS): a utility program for the
802   investigation of equilibria involving soluble and partially soluble
803   species. Coordination Chemistry Reviews 184, 311–318.
804   doi:10.1016/S0010-8545(98)00260-4
805 Arnold, T., Kirk, G.J.D., Wissuwa, M., Frei, M., Zhao, F.-J., Mason, T.F.D.,
806   Weiss, D.J., 2010. Evidence for the mechanisms of zinc uptake by rice
807   using isotope fractionation. Plant, Cell & Environment 33, 370–381.
808   doi:10.1111/j.1365-3040.2009.02085.x
809 Ayers, J.C., Goodbred, S., George, G., Fry, D., Benneyworth, L.,
810   Hornberger, G., Roy, K., Karim, M.R., Akter, F., 2016. Sources of
811   salinity and arsenic in groundwater in southwest Bangladesh.
812   Geochemical Transactions 17, 1–22. doi:10.1186/s12932-016-0036-6
813 Bahar, M.M., Reza, M.S., 2010. Hydrochemical characteristics and quality
814   assessment of shallow groundwater in a coastal area of southwest
815   Bangladesh. Environmental Earth Sciences 61, 1065–1073.
816   doi:10.1007/s12665-009-0427-4
817 Bais, H.P., Weir, T.L., Perry, L.G., Gilroy, S., Vivanco, J.M., 2006. The role
818   of root exudates in rhizosophere interactions with plants and other
819   organisms. Annual Review of Plant Biology 57, 233–266.
820   doi:10.1146/annurev.arplant.57.032905.105159
821 Bertin, C., Yang, X., Weston, L.A., 2003. The role of root exudates and
822   allelochemicals in the rhizosphere. Plant and Soil.
823   doi:10.1023/A:1026290508166
824 Bhowmick, Arjun Chandra, Chakrabarty, T., Akter, S., Saifullah, A.S.M.,
825   Sheikh, M.S., Bhowmick, Arjun C, 2014. Use of fertilizer and
826   pesticide for crop production in Agrarian area of Tangail District,
827   Bangladesh. Environment and Ecology Research 2, 253–261.
828   doi:10.13189/eer.2014.020605
829 Black, A.S., Campbell, A.S., 1982. Ionic strength of soil solution and its
830   effect on charge properties of some New Zealand soils. Journal of Soil
831   Science 33, 249–262. doi:10.1111/j.1365-2389.1982.tb01763.x
832 Bravin, M.N., Tentscher, P., Rose, J., Hinsinger, P., 2009. Rhizosphere pH
833   Gradient Controls Copper Availability in a Strongly Acidic Soil.
834   Environmental Science & Technology 43, 5686–5691.
835   doi:10.1021/es900055k
836 Bretti, C., De Stefano, C., Foti, C., Sammartano, S., 2006. Critical
837   evaluation of protonation constants. Literature analysis and
838   experimental potentiometric and calorimetric data for the
839   thermodynamics of phthalate protonation in different ionic media.
840   Journal of Solution Chemistry 35, 1227–1244. doi:10.1007/s10953-
841   006-9057-6
842 Bretti, C., Foti, C., Sammartano, S., 2004. A new approach in the use of SIT
843   in determining the dependence on ionic strength of activity
844   coefficients. Application to some chloride salts of interest in the
845   speciation of natural fluids. Chemical Speciation and Bioavailability
846   16, 105–110. doi:10.3184/095422904782775036

847   Butler, A., Theisen, R.M., 2010. Iron(III)-siderophore coordination
848   chemistry: Reactivity of marine siderophores. Coordination Chemistry
849   Reviews 254, 288–296. doi:10.1016/j.ccr.2009.09.010
850   Cao, J., Lam, K.C., Dawson, R.W., Liu, W.X., Tao, S., 2004. The effect of
851   pH, ion strength and reactant content on the complexation of Cu2+ by
852   various natural organic ligands from water and soil in Hong Kong.
853   Chemosphere 54, 507–514. doi:10.1016/j.chemosphere.2003.08.027
854   Capone, S., De Robertis, A., De Stefano, C., Sammartano, S., 1986.
855   Formation and stability of zinc(II) and cadmium(II) citrate complexes
856   in aqueous solution at various temperatures. Talanta 33, 763–767.
857   doi:10.1016/0039-9140(86)80184-9
858   Cheah, S.-F., Kraemer, S.M., Cervini-Silva, J., Sposito, G., 2003. Steady-
859   state dissolution kinetics of goethite in the presence of
860   desferrioxamine B and oxalate ligands: implications for the microbial
861   acquisition of iron. Chemical Geology 198, 63–75.
862   doi:10.1016/S0009-2541(02)00421-7
863   Cigala, R.M., Crea, F., De Stefano, C., Foti, C., Milea, D., Sammartano, S.,
864   2015a. Zinc(II) complexes with hydroxocarboxylates and mixed metal
865   species with tin(II) in different salts aqueous solutions at different
866   ionic strengths: Formation, stability, and weak interactions with
867   supporting electrolytes. Monatshefte Fur Chemie 146, 527–540.
868   doi:10.1007/s00706-014-1394-3
869   Cigala, R.M., Crea, F., De Stefano, C., Foti, C., Milea, D., Sammartano, S.,
870   2015b. Zinc(II) complexes with hydroxocarboxylates and mixed metal
871   species with tin(II) in different salts aqueous solutions at different
872   ionic strengths: formation, stability, and weak interactions with
873   supporting electrolytes. Monatshefte Für Chemie - Chemical Monthly
874   146, 527–540. doi:10.1007/s00706-014-1394-3
875   Cigala, R.M., Crea, F., De Stefano, C., Lando, G., Manfredi, G.,
876   Sammartano, S., 2012. Quantitative study on the interaction of
877   Sn2+and Zn2+with some phosphate ligands, in aqueous solution at
878   different ionic strengths. Journal of Molecular Liquids 165, 143–153.
879   doi:10.1016/j.molliq.2011.11.002
880   Cigala, R.M., Crea, F., De Stefano, C., Milea, D., Sammartano, S.,
881   Scopelliti, M., 2013. Speciation of tin(II) in aqueous solution:
882   Thermodynamic and spectroscopic study of simple and mixed
883   hydroxocarboxylate complexes. Monatshefte Fur Chemie 144, 761–
884   772. doi:10.1007/s00706-013-0961-3
885   Codd, R., Richardson-Sanchez, T., Telfer, T.J., Gotsbacher, M.P., 2018.
886   Advances in the Chemical Biology of Desferrioxamine B. ACS
887   Chemical Biology. doi:10.1021/acschembio.7b00851
888   Daniele, P.G., Ostacoli, G., Zerbinati, O., Sammartano, S., De Robertis, A.,
889   1988. Mixed metal complexes in solution. Thermodynamic and
890   spectrophotometric study of copper(II)-citrate heterobinuclear
891   complexes with nickel(II), zinc(II) or cadmium(II) in aqueous
892   solution, Transition Met. Chem.
893   Di Bonito, M., Lofts, S., Groenenberg, J.E., 2018. Models of Geochemical
894   Speciation: Structure and Applications, in: Environmental
895   Geochemistry: Site Characterization, Data Analysis and Case
896   Histories: Second Edition. Elsevier, pp. 237–305. doi:10.1016/B978-
897   0-444-63763-5.00012-4
898   Dolling, P., Ritchie, G., 1985. Estimates of soil solution ionic strength and
899   the determination of pH in West Australian soils. Soil Research 23,
900   309. doi:10.1071/SR9850309
901   Edmeades, D., Wheeler, D., Clinton, O., 1985. The chemical composition
902   and ionic strength of soil solutions from New Zealand topsoils. Soil
903   Research 23, 151. doi:10.1071/SR9850151
904   Farkas, E., Csóka, H., Micera, G., Dessi, A., 1997. Copper(II), nickel(II),
905   zinc(II), and molybdenum(VI) complexes of desferrioxamine B in
906   aqueous solution. Journal of Inorganic Biochemistry 65, 281–286.

907   doi:10.1016/S0162-0134(96)00144-4
908 Field, T.B., Coburn, J., McCourt, J.L., McBryde, W.A.E., 1975.
909   Composition and stability of some metal citrate and diglycolate
910   complexes in aqueous solution. Analytica Chimica Acta 74, 101–106.
911   doi:10.1016/S0003-2670(01)82783-5
912 Gans, P., O'Sullivan, B., 2000. GLEE, a new computer program for glass
913   electrode calibration. Talanta 51, 33–7. doi:10.1016/s0039-
914   9140(99)00245-3
915 Gans, P., Sabatini, A., Vacca, A., 1996. Investigation of equilibria in
916   solution. Determination of equilibrium constants with the
917   HYPERQUAD suite of programs. Talanta 43, 1739–1753.
918   doi:10.1016/0039-9140(96)01958-3
919 Gao, X., Zhang, F., Hoffland, E., 2009. Malate Exudation by Six Aerobic
920   Rice Genotypes Varying in Zinc Uptake Efficiency. Journal of
921   Environment Quality 38, 2315. doi:10.2134/jeq2009.0043
922 Gollany, H.T., Schumacher, T.E., 1993. Combined use of colorimetric and
923   microelectrode methods for evaluating rhizosphere pH. Plant and Soil
924   154, 151–159. doi:10.1007/BF00012520
925 Gries, D., Klatt, S., Runge, M., 1998. Copper-deficiency-induced
926   phytosiderophore release in the calcicole grass Hordelymus
927   europaeus. New Phytologist 140, 95–101. doi:10.1046/j.1469-
928   8137.1998.00250.x
929 Gustafsson, J.P., Visual MINTEQ, version 3.1. 2013
930   https://vminteq.lwr.kth.se
931 Harris, W.R., Raymond, K.N., Weitl, F.L., 1981. Ferric Ion Sequestering
932   Agents. 6. The Spectrophotometric and Potentiometric Evaluation of
933   Sulfonated Tricatecholate Ligands. Journal of the American Chemical
934   Society 103, 2667–2675. doi:10.1021/ja00400a030
935 Hernlem, B.J., Vane, L.M., Sayles, G.D., 1996. Stability constants for
936   complexes of the siderophore desferrioxamine B with selected heavy
937   metal cations. Inorganica Chimica Acta 244, 179–184.
938   doi:10.1016/0020-1693(95)04780-8
939 Hoffland, E., Wei, C., Wissuwa, M., 2006. Organic anion exudation by
940   lowland rice (Oryza sativa L.) at zinc and phosphorus deficiency, in:
941   Plant and Soil. pp. 155–162. doi:10.1007/s11104-005-3937-1
942 Hu, W., Xie, J., Chau, H.W., Si, B.C., 2015. Evaluation of parameter
943   uncertainties in nonlinear regression using Microsoft Excel
944   Spreadsheet. Environmental Systems Research 4, 1–12.
945   doi:10.1186/s40068-015-0031-4
946 Hu, Z., Faucher, S., Zhuo, Y., Sun, Y., Wang, S., Zhao, D., 2015.
947   Combination of Optimization and Metalated-Ligand Exchange: An
948   Effective Approach to Functionalize UiO-66(Zr) MOFs for CO$_2$
949   Separation. Chemistry - A European Journal 21, 17246–17255.
950   doi:10.1002/chem.201503078
951 Hug, S.J., Leupin, O.X., Berg, M., 2008. Bangladesh and Vietnam:
952   Different groundwater compositions require different approaches to
953   arsenic mitigation. Environmental Science and Technology.
954   doi:10.1021/es7028284
955 Ito, H., Fujii, M., Masago, Y., Waite, T.D., Omura, T., 2015. Effect of ionic
956   strength on ligand exchange kinetics between a mononuclear ferric
957   citrate complex and siderophore desferrioxamine B. Geochimica et
958   Cosmochimica Acta 154, 81–97. doi:10.1016/j.gca.2015.01.020
959 Jones, D.L., 1998. Organic acids in the rhizosphere - A critical review. Plant
960   and Soil 205, 25–44. doi:10.1023/A:1004356007312
961 Jones, D.L., Dennis, P.G., Owen, A.G., Van Hees, P.A.W., 2003. Organic
962   acid behavior in soils - Misconceptions and knowledge gaps. Plant
963   and Soil 248, 31–41. doi:10.1023/A:1022304332313
964 Kirk, G.J.D., 1993. Root ventilation, rhizosphere modification, and nutrient
965   uptake by rice, in: Systems Approaches for Agricultural Development.
966   Springer Netherlands, Dordrecht, pp. 221–232. doi:10.1007/978-94-

011-2842-1_13

Krężel, A., Maret, W., 2016. The biological inorganic chemistry of zinc
    ions. Archives of Biochemistry and Biophysics 611, 3–19.
    doi:10.1016/j.abb.2016.04.010

Kumssa, D.B., Joy, E.J.M., Ander, E.L., Watts, M.J., Young, S.D., Walker,
    S., Broadley, M.R., 2015. Dietary calcium and zinc deficiency risks
    are decreasing but remain prevalent. Scientific Reports 5.
    doi:10.1038/srep10974

Li, N.C., Lindenbaum, A., White, J.M., 1959. Some metal complexes of
    citric and tricarballylic acids. Journal of Inorganic and Nuclear
    Chemistry 12, 122–128. doi:10.1016/0022-1902(59)80101-9

Marschner, H., 1988. Mechanisms of Manganese Acquisition by Roots from
    Soils, in: Manganese in Soils and Plants. Springer Netherlands,
    Dordrecht, pp. 191–204. doi:10.1007/978-94-009-2817-6_14

Matsushima, Y., 1963. Determination of Complex Stability Constants by
    Ion Exchange Method. : Extension of Schubert's Method to Lower pH
    Region. Chemical & Pharmaceutical Bulletin 11, 566–570.
    doi:10.1248/cpb.11.566

McRose, D.L., Seyedsayamdost, M.R., Morel, F.M.M., 2018. Multiple
    siderophores: bug or feature? JBIC Journal of Biological Inorganic
    Chemistry 23, 983–993. doi:10.1007/s00775-018-1617-x

Milne, C.J., Kinniburgh, D.G., Van Riemsdijk, W.H., Tipping, E., 2003.
    Generic NICA - Donnan model parameters for metal-ion binding by
    humic substances. Environmental Science and Technology 37, 958–
    971. doi:10.1021/es0258879

Montanarella, L., Pennock, D.J., McKenzie, N., Badraoui, M., Chude, V.,
    Baptista, I., Mamo, T., Yemefack, M., Singh Aulakh, M., Yagi, K.,
    Young Hong, S., Vijarnsorn, P., Zhang, G.-L., Arrouays, D., Black,
    H., Krasilnikov, P., Sobocká, J., Alegre, J., Henriquez, C.R., de
    Lourdes Mendonça-Santos, M., Taboada, M., Espinosa-Victoria, D.,
    AlShankiti, A., AlaviPanah, S.K., Elsheikh, E.A.E.M., Hempel, J.,
    Camps Arbestain, M., Nachtergaele, F., Vargas, R., 2016. World's
    soils are under threat. SOIL 2, 79–82. doi:10.5194/soil-2-79-2016

Northover, G.H.R., Garcia-España, E., Weiss, D.J., 2020. Unravelling the
    modus operandi of phytosiderophores during zinc uptake in rice: the
    importance of geochemical gradients and accurate stability constants .
    Journal of Experimental Botany. doi:10.1093/jxb/eraa580

Powell, K.J., Brown, P.L., Byrne, R.H., Gajda, T., Hefter, G., Sjöberg, S.,
    Wanner, H., 2005. Chemical speciation of environmentally significant
    heavy metals with inorganic ligands. Part 1: The Hg2+– Cl–, OH–,
    CO32–, SO42–, and PO43– aqueous systems (IUPAC Technical
    Report). Pure and Applied Chemistry 77, 739–800.
    doi:10.1351/pac200577040739

Powell, P.E., Cline, G.R., Reid, C.P.P., Szaniszlo, P.J., 1980. Occurrence of
    hydroxamate siderophore iron chelators in soils. Nature 287, 833–834.
    doi:10.1038/287833a0

Ptashnyk, M., Roose, T., Jones, D.L., Kirk, G.J.D., 2011. Enhanced zinc
    uptake by rice through phytosiderophore secretion: A modelling
    study. Plant, Cell and Environment 34, 2038–2046.
    doi:10.1111/j.1365-3040.2011.02401.x

Raynaud, X., 2010. Soil properties are key determinants for the
    development of exudate gradients in a rhizosphere simulation model.
    Soil Biology and Biochemistry 42, 210–219.
    doi:10.1016/J.SOILBIO.2009.10.019

Reichard, P.U., Kretzschmar, R., Kraemer, S.M., 2007. Dissolution
    mechanisms of goethite in the presence of siderophores and organic
    acids. Geochimica et Cosmochimica Acta 71, 5635–5650.
    doi:10.1016/J.GCA.2006.12.022

Rose, T.J., Impa, S.M., Rose, M.T., Pariasca-Tanaka, J., Mori, A., Heuer, S.,
    Johnson-Beebout, S.E., Wissuwa, M., 2013. Enhancing phosphorus

1027   and zinc acquisition efficiency in rice: a critical review of root traits
1028   and their potential utility in rice breeding. Annals of Botany 112, 331–
1029   345. doi:10.1093/aob/mcs217
1030 Schijf, J., Christenson, E.A., Potter, K.J., 2015. Different binding modes of
1031   Cu and Pb vs. Cd, Ni, and Zn with the trihydroxamate siderophore
1032   desferrioxamine B at seawater ionic strength. Marine Chemistry 173,
1033   40–51. doi:10.1016/j.marchem.2015.02.014
1034 Sharma, P., Aggarwal, P., Kaur, A., 2017. Biofortification: A new approach
1035   to eradicate hidden hunger. Food Reviews International 33, 1–21.
1036   doi:10.1080/87559129.2015.1137309
1037 Siddique, M.N.A., Abdullah, 2015. Fertilizer recommendation for
1038   Agriculture: practice, practicalities and adaptation in Bangladesh and
1039   Netherlands. Int. J. Bus. Manag. Soc. Res 01, 21–40.
1040   doi:10.18801/ijbmsr.010115.03
1041 Smith, R.M., Martell, A.E., Motekaitis, R.J., 2004. N IST Standard
1042   Reference Database 46 NIST Critically Selected Stability Constants of
1043   Metal Complexes Database Version 8.0 For Windows Users' Guide.
1044 Tufano, T.P., Raymond, K.N., 1981. Coordination Chemistry of Microbial
1045   Iron Transport Compounds. 21. Kinetics and Mechanism of Iron
1046   Exchange in Hydroxamate Siderophore Complexes. Journal of the
1047   American Chemical Society 103, 6617–6624.
1048   doi:10.1021/ja00412a015
1049 Weston, L.A., Ryan, P.R., Watt, M., 2012. Mechanisms for cellular
1050   transport and release of allelochemicals from plant roots into the
1051   rhizosphere. Journal of Experimental Botany 63, 3445–3454.
1052   doi:10.1093/jxb/ers054
1053 Weiss, D., Northover, G, Garcia-Espana, 2021. Isotope fractionation and the
1054   possible role of 2'deoxymugineic acid during scavenging and uptake
1055   of zinc in the rhizosphere. Chemical Geology. *Under review*
1056 Wheeler, T., Braun, J. von, 2013. Climate Change Impacts on Global Food
1057   Security. Science 341, 508–513. doi:10.1126/SCIENCE.1239402
1058 Widodo, J.A., Broadley, M.R., Rose, T., Frei, M., Pariasca-Tanaka, J.,
1059   Yoshihashi, T., Thomson, M., Hammond, J.P., Aprile, A., Close, T.J.,
1060   Ismail, A.M., Wissuwa, M., 2010. Response to zinc deficiency of two
1061   rice lines with contrasting tolerance is determined by root growth
1062   maintenance and organic acid exudation rates, and not by zinc-
1063   transporter activity. New Phytologist 186, 400–414.
1064   doi:10.1111/j.1469-8137.2009.03177.x
1065 Zhang, F.-S., Römheld, V., Marschner, H., 1991. Diurnal rhythm of release
1066   of phytosiderophores and uptake rate of zinc in iron-deficient wheat.
1067   Soil Science and Plant Nutrition 37, 671–678.
1068   doi:10.1080/00380768.1991.10416935
1069 Zhong, L., Yang, J., Liu, L., Li, X., 2013. Desferrioxamine-B promoted
1070   dissolution of an Oxisol and the effect of low-molecular-weight
1071   organic acids. Biology and Fertility of Soils 49, 1077–1083.
1072   doi:10.1007/s00374-013-0803-9

9. Tables

Table 1. Ligand acidity constants (log β) at different ionic strength (M NaCl), $T = 298.1$ K.

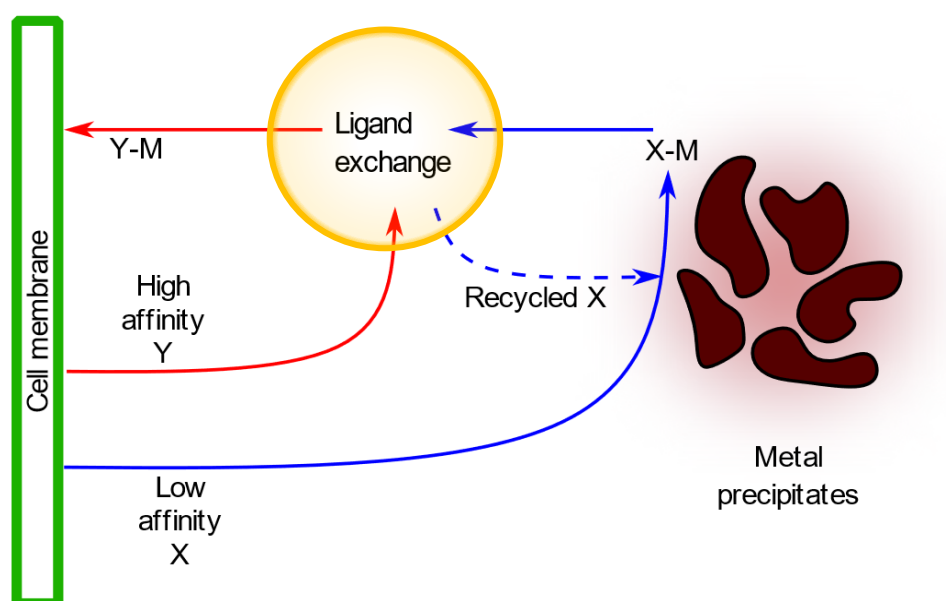| Ligand	Equilibrium	0.05	0.15	0.3	0.5	1	log β^0	C
Citrate	$H^+ + Cit^{3-} = HCit^{2-}$	5.69±0.01	5.44±0.01	5.35±0.01	5.26±0.01	5.12±0.01	6.195±0.001	0.194±0.001
	$2H^+ + Cit^{3-} = H_2Cit^-$	10.18±0.02	9.57±0.02	9.45±0.02	9.32±0.02	9.13±0.02	10.911±0.005	0.301±0.012
	$3H^+ + Cit^{3-} = H_3Cit$	13.00±0.05	12.10±0.03	11.94±0.04	11.70±0.03	11.53±0.03	13.789±0.006	0.184±0.180
DFOB	$H^+ + DFOB^{3-} = HDFOB^{2-}$	11.07±0.07	10.74±0.04	10.36±.02	10.35±0.02	10.14±0.06	11.491±0.002	-0.169±0.003
	$2H^+ + DFOB^{3-} = H_2DFOB^-$	20.94±0.09	20.25±0.06	19.84±0.04	19.77±0.04	19.77±0.08	21.530±0.006	0.173±0.011
	$3H^+ + DFOB^{3-} = H_3DFOB$	30.05±0.12	29.10±0.09	28.61±0.07	28.60±0.08	28.57±0.12	30.691±0.012	0.194±0.028
	$4H^+ + DFOB^{3-} = H_4DFOB^+$	38.83±0.14	37.46±0.13	37.00±0.10	36.97±0.16	36.92±0.14	39.250±0.023	-0.079±0.043

10. Figures

Figure 1. Conceptual model of interplay between weak (X) and strong (Y) ligands released by bacteria as suggested by McRose *et al.* (2018). Formation of an MX (where M = metal) complex strips M from the metal precipitates and brings M into solution; M is exchanged between X and Y; Y transports M towards cell surface whilst X is free to return to the metal precipitates. A key question that arises is what triggers the ligand exchange?
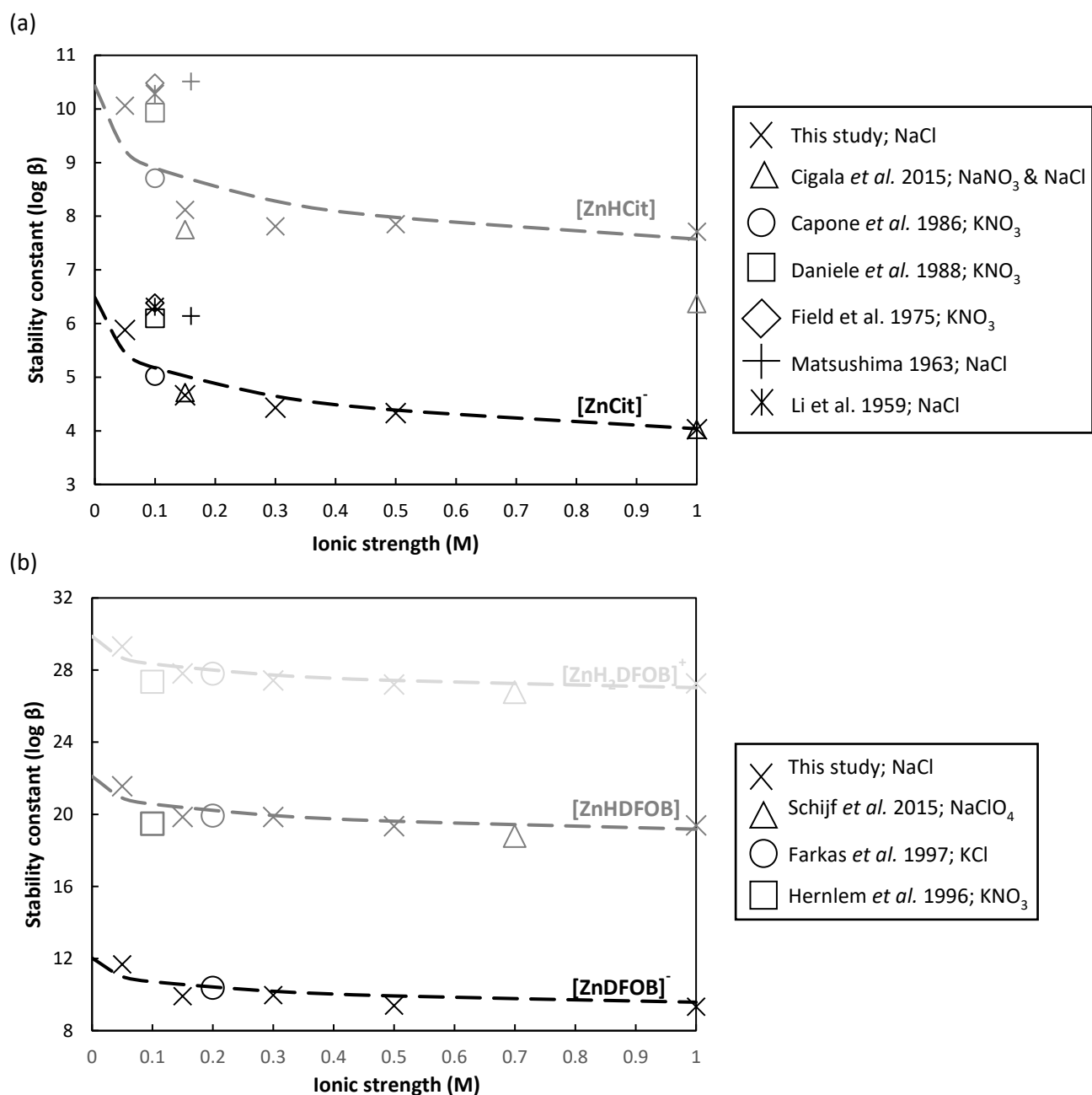
Figure 2. Experimental zinc(II)-ligand stability constants for **(a)** citrate and **(b)** DFOB. For each species, the modified Extended Debye-Hückel model has been parameterised using experimental data from this study and is shown as a dashed line. Literature data is included in the figure for comparison. Comprehensive results for the zinc(II)/ligand systems, including stability constants for hydrolysed zinc(II)-ligand species, are reported in Table S1.
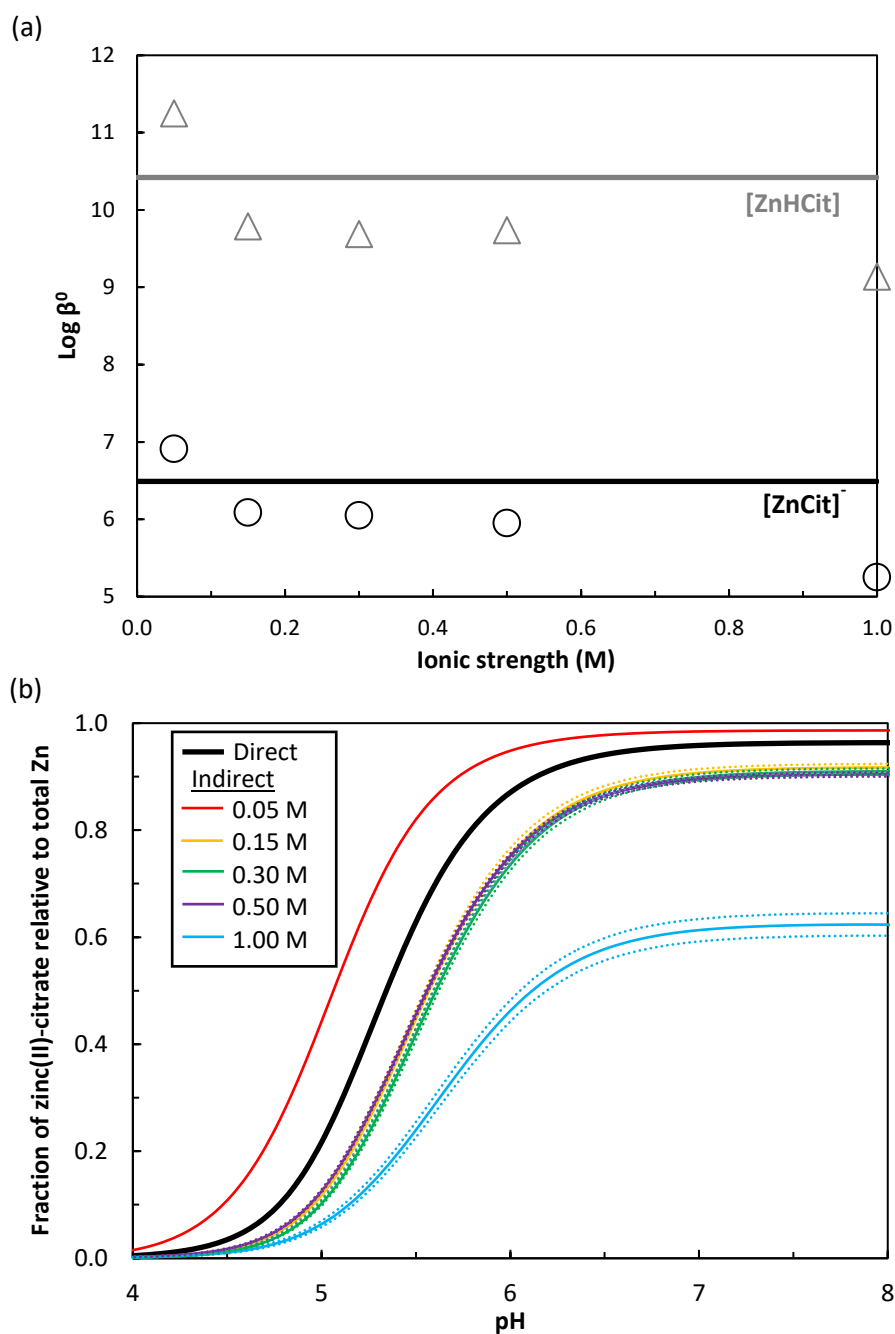
Figure 3. (a) Intrinsic stability constants for the formation of [ZnCit]⁻ and [ZnHCit] species determined at different ionic strengths using the Davies equation are shown as circles and triangles, respectively. The intrinsic stability constants for the same two species determined by fitting the modified version of the Extended Debye-Hückel equation to the full ionic strength dataset are shown as solid lines (b) Fraction of complexed zinc(II) in a [Zn] = 10⁻⁶ M and [citrate] = 10⁻⁵ M system modelled at infinite dilution using intrinsic stability constants determined (i) directly, by fitting the modified version of the Extended Debye-Hückel equation to the full citrate (pK_a and zinc(II)-citrate) stability constant dataset (ii-vi) indirectly, using the Davies equation to calculate activity coefficients and adjusting the citrate (pK_a and zinc(II)-citrate) stability constants separately at 0.05, 0.15, 0.30, 0.50, and 1.00 M (Table S2). The dashed lines show the error on the respective curves. The error was calculated by re-running the analysis, starting with the high/low estimates for the experimental stability constants. For the direct and 0.05 M indirect models, the error was too small to display.
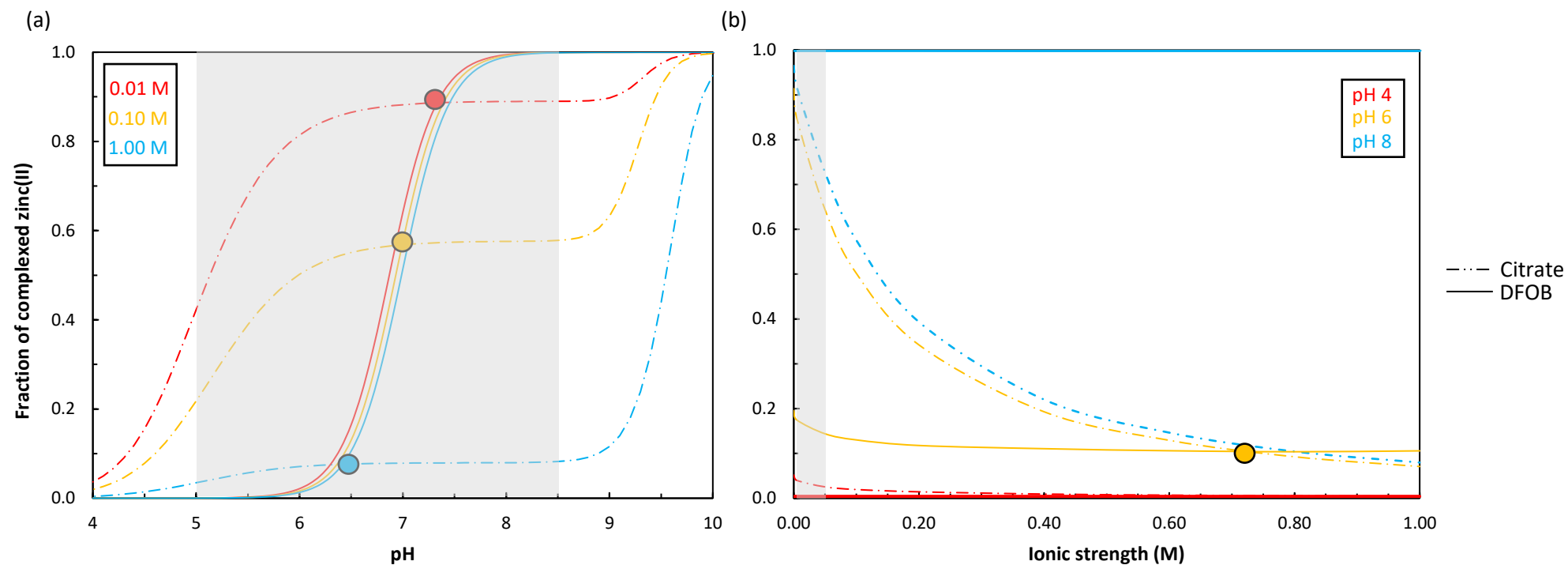
Figure 4. Fraction of complexed zinc(II) in our representative zinc(II)/LMWOA (citrate) and zinc(II)/siderophore (DFOB) systems ([Zn] = 10^{-6} M and [L] = 10^{-5} M) as a function of **(a)** pH and **(b)** ionic strength in NaCl solutions. The shaded grey area shows the rhizosphere-relevant pH and ionic strength zones. The raw data for these plots is supplied in the supporting information (Table S3-S4).
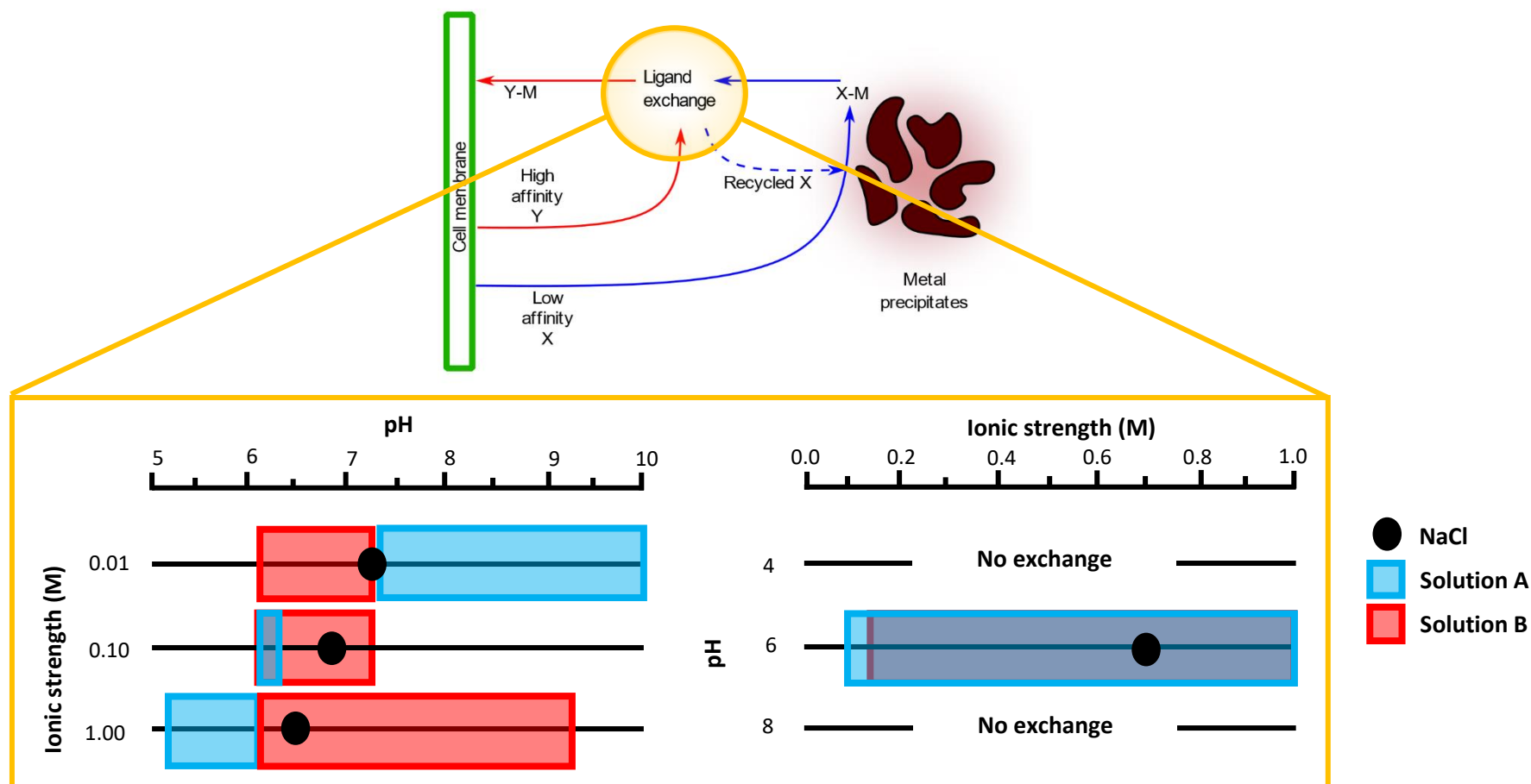
Figure 5. Calculated LIPs for the exchange of zinc(II) between our representative LMWOA and siderophore in two model solutions based on the chemistry of rice-growing soils. The two model solutions are differentiated by the concentration of bicarbonate ions; solution A = 2 mM and solution B = 8 mM. The predicted LIPs from the analysis in NaCl using standard [Zn] and [L] are included for comparison. The LIPs calculated for solution A and B are reported as ranges because different sets of LMWOA (1 – 50 μM) and siderophore (0.1 – 1 μM) concentrations were analysed in each of the solutions.